JOURNAL OF PROPULSION AND POWER
Vol. 27, No. 4, July–August 2011

Model of Ideal Electrohydrodynamic Thruster

L. Pekker*
ERC, Inc., Edwards Air Force Base, California 93524
and
M. Young†
U.S. Air Force Research Laboratory, Edwards Air Force Base, California 93524

DOI: 10.2514/1.B34097

The idea of using the electrohydrodynamic ionic wind pump effect in thruster applications is theoretically examined. Although this idea has been under discussion for many decades, there is still no commonly accepted view on electrohydrodynamic thrusters: for example, whether electrohydrodynamic thrusters are worthwhile, what level of thrust and thrust efficiency can be obtained from electrohydrodynamic thrusters, etc. In this paper, a simple one-dimensional model of an ideal electrohydrodynamic thruster for calculating thrust efficiency and thrust of electrohydrodynamic thrusters is presented. The maximum current that can be achieved for an ideal electrohydrodynamic thruster at a given voltage is also calculated. This allows the calculation of the maximum thrust that can be obtained from the thruster and the corresponding thrust efficiency. It is shown that, with an increase in the voltage, the maximum thrust and the corresponding thrust efficiency move in opposite directions: the thrust efficiency decreases, while the thrust increases. It is also shown that, at high altitudes, the performance of electrohydrodynamic thrusters (thrust and thrust efficiency) drops very fast; therefore, using electrohydrodynamic thrusters at altitudes greater than 5 km is apparently unrealistic. The model shows that maximum thrust cannot exceed 20–30 N/m^2 at sea level, even at breakdown voltage. The model illuminates the physical limitations of electrohydrodynamic thrusters and provides reasonable estimates of the performance limits of real electrohydrodynamic thrusters.

Nomenclature

A, B	=	calculated constants
C_D	=	drag coefficient
E	=	magnitude of electrical field
e	=	electron charge
E_0	=	magnitude of electrical field at anode
H	=	altitude above sea level
i	=	index corresponding to ith spatial step
j	=	electrical current density
$j_{\max}$	=	maximum space-charge-limited current density
k	=	Boltzmann constant
L	=	discharge length of thruster
M_i	=	$\mu_i \cdot n_a$
m_a	=	mass of neutral gas molecule
m_i	=	mass of ion
n_a	=	neutral gas number density
$n_{a,0}$	=	neutral gas number density at anode
n_i	=	ion number density
P	=	gas pressure
S	=	effective cross section of aircraft
T	=	thrust per unit area of discharge
T_a	=	temperature of neutral gas flow
T_i	=	ion temperature
$T_{\max}$	=	maximum thrust per unit area of discharge
U	=	discharge voltage
u	=	velocity of neutral gas flow in thruster coordinate system
U_0	=	given discharge voltage
u_0	=	incoming velocity of neutral gas flow at anode
u_1	=	exit velocity of neutral gas flow at cathode
V_{drift}	=	ion drift velocity
$V_{\text{drift},0}$	=	ion drift velocity at anode
V_{Ta}	=	thermal velocity of neutral gas flow
W_j	=	electrical power deposited in discharge per unit area of discharge
W_k	=	gain of kinetic energy of gas flow per second per unit area of discharge
$W_{k,i}$	=	kinetic energy of ion flow per unit area of discharge
x	=	axis directed along thruster
ΔT_a	=	increase of gas temperature in thruster due to ohmic heating
ΔV	=	change in velocity
Δx	=	spatial step
ε_0	=	permittivity of free space
λ_{ia}	=	ion-neutral collision length
μ_i	=	ion mobility
ρ	=	air mass density
ρ_H	=	air mass density at altitude H
ρ_{sl}	=	air mass density at sea level
τ_{in}	=	ion-neutral collision time
χ	=	thruster efficiency
χ_H	=	thruster efficiency at altitude H
χ_{sl}	=	thruster efficiency at sea level

Received 27 August 2010; revision received 23 December 2010; accepted for publication 31 December 2010.

*Senior Research Staff Engineer; leonid.pekker.ctr@edwards.af.mil.
†Program Manager, Advanced Concepts Group; marcus.young@edwards.af.mil.

I. Introduction

ELECTROHYDRODYNAMICS (EHD), or alternatively, electrofluid dynamics or electrokinetics, refers to motion of electrically charged fluids under the influence of applied electric fields. In EHD thrusters, the applied electric field accelerates the electrically charged particles while collisional coupling between the charged particles and neutral particles is used to convert the directed energy of the charged particles into neutral gas/fluid particle flow without the need for moving parts (Fig. 1). Since the momentum transfer between ions and neutral particles is much more efficient than between electrons and neutral particles, neutral gas flows produced in EHD devices are commonly referred to as ion wind (also ionic wind, ion-driven wind, corona wind, electric wind, and others) flows. The EHD ionic wind pump effect was discovered in 1709 by

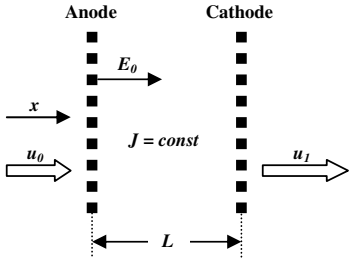

Fig. 1 Schematic (not to scale) of EHD thruster.

Hauksbee [1] and later investigated by numerous scientists, including Newton, Faraday, and Maxwell; a history of EHD ionic wind pump effect can be found in an excellent review by Robinson [2]. The predominantly neutral gas flows produced using the EHD pump effect have been successfully incorporated into a variety of practical devices. The most prominent application is currently ionic air purifiers such as the Ionic Breeze [3]. Such devices use the ion wind effect to drive untreated air through the device and hit a collection plate where the unwanted particles stick to the plate's surface to remove them by the air flow. Another, more recent, application is EHD laptop-cooling fans. Jewell-Larsen et al. [4] have demonstrated that such devices can achieve similar cooling performance as the existing high-revolution-per-minute cooling fans but at reduced noise levels. In 1961, Steutzer [5] investigated theoretically and experimentally operating the EHD ion wind devices backward as high-voltage generators, where the ion current is generated by friction with liquid flow.

EHD-based propulsion systems for low-speed aircraft were proposed and investigated in the early 1960s. The most prominent effort, called the Ionocraft and led by Major de Seversky, made the front cover of *Popular Mechanics* in August 1964 [6]. The article described the technology as a magic carpet that was viable over the entire range of speeds, up to and including jet aircraft speeds. It also claimed that it would become more efficient than propellers or jets for aircraft propulsion and be able to operate at altitudes as high as 60 miles. One envisioned application was an Ionocraft as large as a city block used as an antimissile platform that would indefinitely stay in the upper atmosphere. At the time of the article, however, the engineers [6] had built only a rudimentary device out of balsa wood, aluminum wire, and an electrical tether down to a high-voltage power supply. They also achieved very limited performance: it took 90 W (30 kV, 3 mA) to lift 2 oz. At that time, they stated that their active work was focused on increasing the energy efficiency.

The serious theoretical and experimental investigation of EHD thrusters began with the work of Christenson and Moller [7], in which they developed a one-dimensional (1-D) model of EHD propulsion systems and compared it with experiments. Experimentally, they achieved a thruster efficiency (conversion efficiency from electrical energy to fluid kinetic energy) that was about one half of the values predicted by the model. They concluded that approximately 90% of the input energy ended up as flow thermal energy and that the ion mobility of air would have to be reduced by about two orders of magnitude for realistic applications. In their theoretical analysis, the authors have assumed that the ion mobility is constant and independent of gas density. Although in general, this assumption is inaccurate (it works only when $\Delta V \to 0$), their model gives reasonable estimates of the magnitude of the thrust and the thrust efficiency. We also would like point out the work of Robinson [8] (which was inaccessible to the public for a long time), where in 1961, he had already developed a model that was very similar to that of Christenson and Moller [7]; in his model, he has also included losses specific to the corona discharge. Robinson came to the same conclusion as Christenson and Moller [7] that the conversion efficiency of EHD ion wind blowers (or EHD thrusters) is very low. He also has pointed out that, in certain gases, the generation of extraneous gases in the corona discharge (e.g., ozone in air) can be a significant limitation of using corona discharge in EHD blowers. In 1986, Bondar and Bastien [9] analytically estimated thruster efficiency and showed that the efficiency increases with fluid velocity. They have experimentally achieved a conversion efficiency of up to 7.5% by operating with an incoming flow velocity of 50 m/s, which was close to their estimated value. In 2005, Singhal and Garimella [10] constructed a transient three-dimensional coupled EHD/Navier–Stokes code and used it to model the effect of incoming neutral gas velocity on the efficiency of EHD pumps (or EHD thrusters). Like Bondar and Bastien [9], they concluded that significant increases in conversion efficiency of EHD pumps are possible by increasing the incoming velocity into the EHD pumps. In recent work, [11] the authors have shown that the exhaust velocity can be increased by adding multiple stages of EHD thrusters in series. They demonstrated a maximum axial velocity for a single-stage 2.5-cm-diam device of 4.5 m/s. They also tested up to seven stages in series, yielding a maximum velocity of over 7 m/s but at a conversion efficiency of around 0.1%.

Thus, the primary limitation of EHD-based propulsion systems is that they are typically very inefficient in terms of thrust efficiency when operating on gases, roughly 1–10%, while competing technologies like fans can achieve χ of 60–70% [8]. There are, however, other factors that could limit the applicability of EHD-based propulsion systems. One of them is that the ion current is space charge limited [7,8], a fact that leads to small ionization fractions in EHD thrusters, typically on the order of 10^{-10} at 1 atm of air pressure. This indicates that space charge buildup in the EHD thruster chambers may limit the amount of achievable thrust per unit area. Other factors, such as local humidity and subtle electrode alignment changes, greatly affected the maximum attainable ion wind velocity [11], indicating that EHD propulsion systems may not be very robust. Obviously, many other factors can negatively impact the performance of EHD thrusters. However, there is still no commonly accepted view on the EHD thruster: e.g., whether an EHD thruster is worthwhile, what level of thrust and thrust efficiency can be obtained from EHD thrusters, etc. Therefore, the construction of an ideal model of EHD thrusters is very important for understanding major physical limitations of EHD thrusters in ideal situations.

In this paper, we present a simple 1-D model of an ideal EHD thruster. A description of the model and numerical results are presented in Secs. II and III, respectively, and conclusions are given in Sec. IV.

II. Description of Model

A schematic of an ideal EHD thruster is shown in Fig. 1. The ions are seeded at the anode and are neutralized at the cathode. Here, we do not consider the mechanism for creating (seeding) the ions. They can be created, for example, by corona discharge at the anode or by other means. The neutral gas flow is coming from the anode side of the thruster. Because of the viscous forces between the neutral gas particles and the ions, the neutral gas flow is accelerated, producing thrust as in a conventional air turbine jet.

In the model, we have made the following assumptions (Fig. 1):

1) The width of the thruster is much larger than the length of the thruster L.

2) All parameters of incoming neutral gas and ion flow are uniform across the thruster.

3) The anode and the cathode are transparent to the neutral gas flow.

4) There are no electrons in the discharge region.

5) All parameters of the thruster are independent of time (i.e., we assume the steady-state regime of thruster operation).

6) The temperature of neutral gas flow in the discharge chamber is constant.

The sixth assumption relies on the assumption that the electrical power put into the discharge is relatively small so that the heating of the gas flow due to the discharge can be ignored. It follows from the first three assumptions that our model is 1-D.

The equations describing the 1-D thruster (Fig. 1) are

$$\varepsilon_0 \cdot \frac{\mathrm{d}E}{\mathrm{d}x} = -e \cdot n_i \tag{1}$$

$$j = e \cdot n_i \cdot (u + V_{\text{drift}}) = \text{const} \tag{2}$$

$$n_{a,0} \cdot u_0 = n_a \cdot u \tag{3}$$

$$m_a \cdot n_{a,0} \cdot u_0 \cdot \frac{\mathrm{d}u}{\mathrm{d}x} = n_i \cdot e \cdot E \tag{4}$$

where Eq. (1) is Poisson's equation, Eq. (2) is the electrical charge conservation law, Eq. (3) is the mass conservation law for neutral particles, Eq. (4) is the momentum conservation law for neutral particles, and

$$V_{\text{drift}} = \mu_i \cdot E \tag{5}$$

$$\mu_i = \frac{e \cdot \tau_{\text{in}}}{m_i} = \frac{M_i}{n_a} \tag{6}$$

In Eq. (2), we have assumed that the ion-neutral collision mean free path is much smaller than L; therefore, the ion velocity without the electric field has to be about equal to the local velocity of gas flow. It should be stressed that in the case where a corona discharge is used to ionize the incoming gas flow, Eq. (2) is exact. In the model, we also assume that M_i is a constant. This is a reasonable assumption as long as the relative velocity between the gas flow and the ion wind V_{drift} is smaller than the neutral particle thermal velocity V_{Ta}, and the temperature of gas flow T_a does not change significantly in the discharge region of the EHD thruster (assumption 6). It should be stressed that, in the case of strong electric fields, when the energy that an ion gains from the electric field between collisions is comparable to the thermal energy of the neutral gas [V_{drift} calculated by Eq. (5) becomes larger than V_{Ta}], the ion drift cannot be described by Eq. (5) any longer [12]. It is worth noting that this situation corresponds, in particular, to the case of the electrical breakdown in gasses. The system of Eqs. (1–6) is essentially the system of equations used by Christensen and Moller [7], however, taking into account dependence of ion mobility on density of neutral gas.

Integrating Eq. (4) along the discharge region, we obtain an equation for the thrust per unit of area of the discharge:

$$T = m_a \cdot n_{a,0} \cdot u_0 \cdot (u_1 - u_0) = e \cdot \int_0^L n_i \cdot E \cdot \mathrm{d}x \tag{7}$$

Multiplying Eq. (4) by u and then integrating along the discharge region, we obtain an equation for the gain of kinetic energy of gas flow per second per unit of area of the discharge:

$$W_k = m_a \cdot n_{a,0} \cdot u_0 \cdot \left(\frac{u_1^2}{2} - \frac{u_o^2}{2}\right) = \int_0^L n_i \cdot e \cdot E \cdot u \cdot \mathrm{d}x \tag{8}$$

The electrical power deposited in the discharge per unit area of the discharge can be calculated as

$$W_j = j \cdot \int_0^L E \cdot \mathrm{d}x = j \cdot U \tag{9}$$

where

$$U = \int_0^L E \cdot \mathrm{d}x \tag{10}$$

Substituting n_i from Eq. (2), E from Eq. (5), μ_i from Eq. (6), and n_a from Eq. (3) into Eqs. (1) and (4) and using algebra, the system of Eqs. (1–6) reduces to the following system of two ordinary differential equations:

$$\frac{\mathrm{d}V_{\text{drift}}}{\mathrm{d}x} = B \cdot \frac{V_{\text{drift}}^2}{(V_{\text{drift}} + u) \cdot u^2} - A \cdot \frac{u}{(V_{\text{drift}} + u)} \tag{11}$$

$$\frac{\mathrm{d}u}{\mathrm{d}x} = B \cdot \frac{V_{\text{drift}}}{(V_{\text{drift}} + u) \cdot u} \tag{12}$$

where A and B are constants:

$$A = \frac{j \cdot M_i}{\varepsilon_0 \cdot n_{a,0} \cdot u_0} \quad \text{and} \quad B = \frac{j}{M_i \cdot m_a} \tag{13}$$

The physical parameters for the thruster are the incoming air velocity and applied voltage. Therefore, we have numerically solved Eqs. (11–13) with two boundary conditions:

$$u(x = 0) = u_0 \quad \text{and} \quad U = U_0 \tag{14}$$

In our algorithm, we solve Eqs. (11–13) for initial values of u and V_{drift} at $x = 0$, u_0, and $V_{\text{drift},0}$, and then iterated $V_{\text{deift},0}$ to satisfy the second boundary condition in Eq. (14).

Now, let us consider the case where the ion's drift velocity is much larger than the velocity of neutral gas flow:

$$V_{\text{drift}} \gg u \tag{15}$$

Dropping u in Eq. (2), we obtain the following equation for E:

$$\varepsilon_0 \cdot \frac{\mathrm{d}E}{\mathrm{d}x} = -\frac{j}{\mu_i \cdot E} \tag{16}$$

Assuming further that $\mu_i = \text{const}$ and solving Eq. (16) analytically for given j and E_0, we obtain the following analytical expressions for $E(x)$, $n_i(x)$, U, and $j_{\max}$:

$$E = E_0 \left[1 - \frac{x}{L} \cdot \left(\frac{j}{j_{\max}}\right)\right]^{1/2} \tag{17}$$

$$n_i = \frac{j}{e \cdot \mu_i \cdot E_0} \left[1 - \frac{x}{L} \cdot \left(\frac{j}{j_{\max}}\right)\right]^{-1/2} \tag{18}$$

$$U = \frac{2}{3} \cdot E_0 \cdot L \cdot \frac{j_{\max}}{j} \left[1 - \left(1 - \frac{j}{j_{\max}}\right)^{3/2}\right] \tag{19}$$

where

$$j_{\max} = \frac{\varepsilon_0 \cdot \mu_i \cdot E_0^2}{2 \cdot L} = \frac{9 \cdot \varepsilon_0 \cdot \mu_i \cdot U^2}{8 \cdot L^3} \tag{20}$$

It follows from Eq. (17) that the current cannot exceed the maximum space-charge-limited current $j_{\max}$: the Child–Langmuir law. In the case when $j \to 0$, we obtain that $U = E_0 \cdot L$ and $n_i = 0$, and when $j = j_{\max}$, Eq. (19) yields $U = \frac{2}{3} \cdot E_0 \cdot L$. Substituting Eqs. (17–19) into Eqs. (7) and (8) and setting u to u_0 in the right-hand side of Eq. (8), we obtain analytical estimates for the thrust per unit area of the discharge and thrust efficiency:

$$T \approx \frac{j \cdot L}{\mu_i} \tag{21}$$

$$\chi = \frac{W_k}{W_j} \approx \frac{u \cdot L}{\mu_i \cdot U} \approx \frac{u}{V_{\text{drift}}} \tag{22}$$

Substituting $j_{\max}$ [Eq. (20)] into Eq. (21), we obtain an estimate for the maximum T that can be achieved from the thruster:

$$T_{\max} \approx \frac{j_{\max} \cdot L}{\mu_i} = \frac{9 \cdot \varepsilon_0 \cdot U^2}{8 \cdot L^2} \tag{23}$$

As one can see from Eq. (23), the maximum thrust is independent of ion mobility when $V_{\text{drift}} \gg u$. It follows from Eqs. (22) and (23) that, with an increase in the thruster voltage, $T_{\max}$ increases while χ decreases. This shows that achieving both targets, high thrust and high thrust efficiency, at once can be difficult.

III. Numerical Results

The exact calculation of ion drift mobility in air is a very complicated task; notably, it depends on ion composition, humidity

of air, pressure, and other factors. Direct measurements of air ion mobility at 1 atm [13] give $\mu_i \approx 1.39 \cdot 10^{-4}$ m^2/(V · s) with a standard deviation of $0.1 \cdot 10^{-4}$ m^2/(V · s). Since the ion mobility of N_2^+ in pure nitrogen gas at a pressure of 1 atm and a temperature of 300 K is $1.37 \cdot 10^{-4}$ m^2/(V · s) [12] and close to the measured average ion mobility of air, we consider in our paper the case of pure nitrogen gas. In our calculations, we have used $M_i = 1.27 \cdot 10^{24}$ 1/(V · s · m) that corresponds to drift of ions N_2^+ in nitrogen gas at a gas temperature of 300 K. Since M_i is weakly dependent on the temperature [$M_i = 1.01 \cdot 10^{24}$ 1/(V · s · m) at 1000 K], our assumption that $M_i = \text{const}$ is well satisfied.

Figures 2–13 present results obtained by numerically solving the system of Eqs. (11–14) at maximum current (maximum thrust). Figure 2 shows maximal current densities vs voltage for different velocities of neutral gas flow u_0; in our model, u_0 can be interpreted as the speed of the aircraft. As expected, with an increase in applied voltage, $j_{\max}$ increases rapidly. As shown in Fig. 3, the maximum thrust of the EHD thruster increases with an increase in the voltage (as expected) and seems not to depend greatly on the speed of the vehicle, as in the case of $V_{\text{drift}} \gg u$ [Eq. (23)]. Figure 4 shows that thruster efficiency increases with an increase in the speed of the vehicle and decreases with an increase in the applied voltage; these trends agree with an estimate of χ for the case of $V_{\text{drift}} \gg u$ [Eq. (22)] and qualitatively agree with the Bondar–Bastien model [9] (Fig. 13).

To investigate how the length of the EHD thruster affects the thruster performance, we have calculated parameters of the EHD thruster for $u_0 = 50$ m/s and $L = 1$ m for different $j_{\max}$ (Figs. 5–10). As shown in Fig. 5, the discharge voltage increases very nonlinearly with the length of the capillary for a fixed magnitude of $j_{\max}$. This behavior of U vs L can be explained by significant nonlinear dependencies of E on x for currents close to $j_{\max}$; an analytical expression of $E(x)$ for the case of $V_{\text{drift}} \gg u$ is shown in Eq. (17). With an increase in L, the thrust increases (Fig. 6), but the thrust efficiency decreases (Fig. 7). We have also calculated ΔV, one of the important parameters of thruster performance (Fig. 8). As one can see, ΔV reaches about 4.5 m/s for $L = 100$ cm and

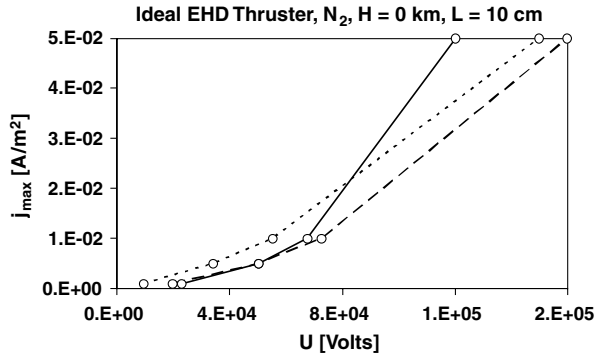

Fig. 2 Maximum current (solid line: $u_0 = 3$ m/s; dashed line: $u_0 = 10$ m/s; dotted line: $u_0 = 50$ m/s).

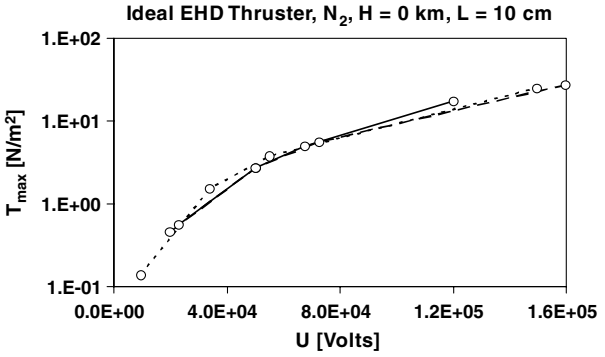

Fig. 3 Thrust at maximum current (solid line: $u_0 = 3$ m/s; dashed line: $u_0 = 10$ m/s; dotted line: $u_0 = 50$ m/s).

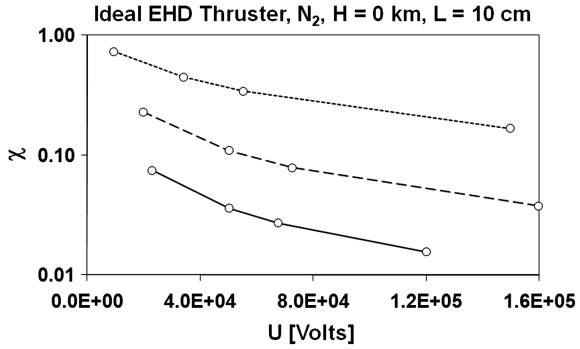

Fig. 4 Thrust efficiency at maximum current (solid line: $u_0 = 3$ m/s; dashed line: $u_0 = 10$ m/s; dotted line: $u_0 = 50$ m/s).

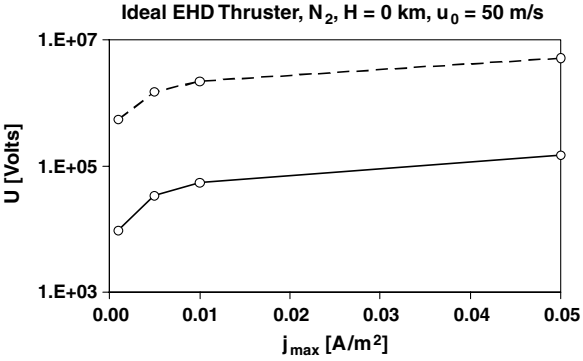

Fig. 5 Voltage at maximum current (solid line: $L = 10$ cm; dashed line: $L = 100$ cm).

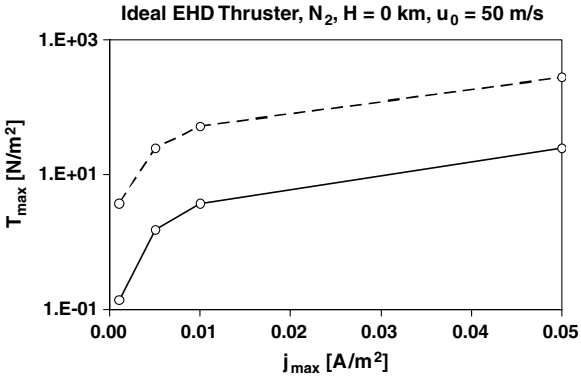

Fig. 6 Thrust at maximum current (solid line: $L = 10$ cm; dashed line: $L = 100$ cm).

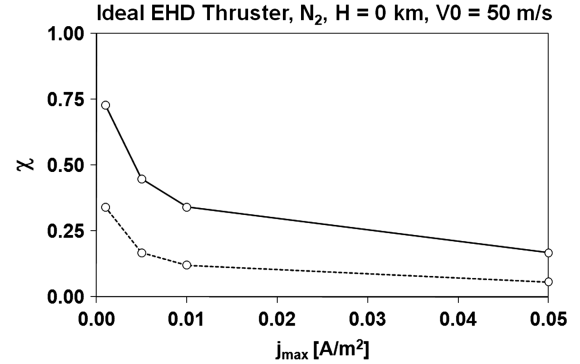

Fig. 7 Thrust efficiency at maximum current (solid line: $L = 10$ cm; dashed line: $L = 100$ cm).

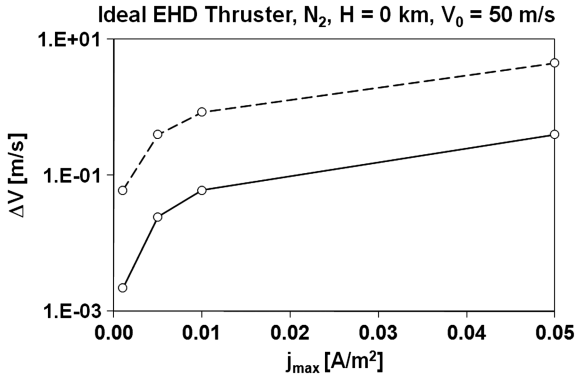

Fig. 8 Change of velocity at maximum current (solid line: $L = 10$ cm; dashed line: $L = 100$ cm).

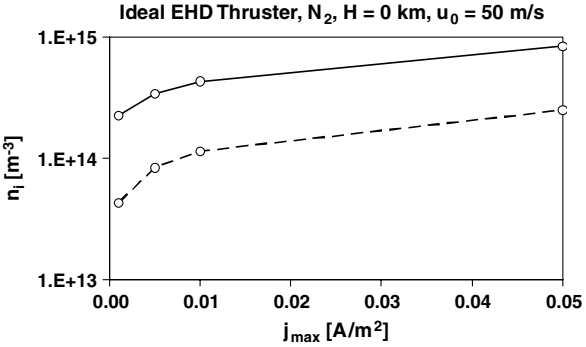

Fig. 9 Ion density at maximum current (solid line: $L = 10$ cm; dashed line: $L = 100$ cm).

$j_{\max} = 0.05$ A/m^2. Since the ion current cannot exceed the space-charge-limited current $j_{\max}$, the ion density in the discharge is very small (Fig. 9).

To investigate the performance of the thruster at different altitudes, we have also calculated the thrust and thruster efficiency for $H = 20$ km. As shown in Figs. 10 and 11, both thrust and thrust efficiency decrease with an increase in H. The reason is that ion mobility increases with a decrease in gas density [Eq. (6)], leading to a decrease in $T_{\max}$ and χ. Now, let us estimate thrust efficiency for a low-speed aircraft powered by an EHD thruster. For low-speed aircraft in steady level flight, the thrust is approximately proportional to the lift force and, therefore, can be considered to be constant (i.e., independent of H) and written as

$$\text{thrust} = \tfrac{1}{2} \cdot \rho \cdot u^2 \cdot S \cdot C_D = \text{const} \tag{24}$$

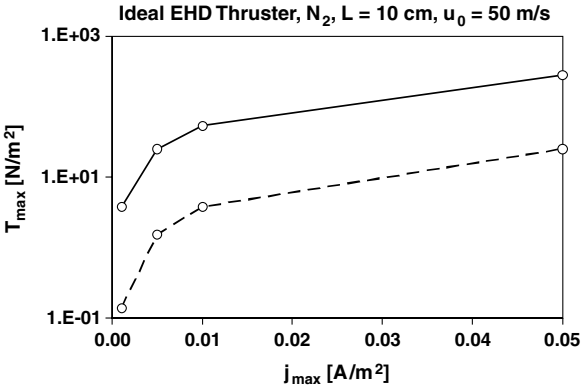

Fig. 10 Thrust at maximum current (solid line: $H = 0$ km; dashed line: $H = 20$ km).

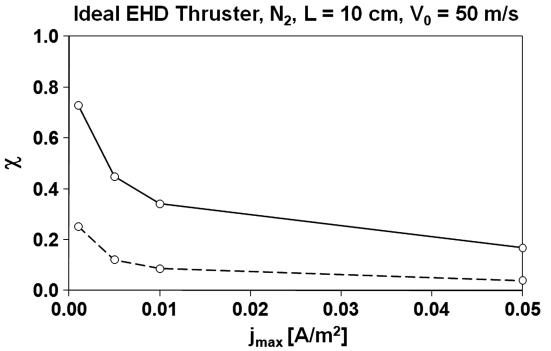

Fig. 11 Thrust efficiency at maximum current; solid line (solid line: $H = 0$ km; dashed line: $H = 20$ km).

where ρ is the air density, u is the velocity of the aircraft, S is the effective cross section of the aircraft, and C_D is the drag coefficient. As one can see, Eq. (24) states that thrust is equal to the drag force. Let ρ_{sl} and u_{sl} be the air density and aircraft velocity at sea level, and let ρ_H and u_H refer to those parameters at altitude H; then, using Eq. (24), we obtain

$$u_H = u_{\text{sl}} \cdot \sqrt{\frac{\rho_{\text{sl}}}{\rho_H}} \tag{25}$$

On the other hand, the thrust provided by an EHD thruster at maximum current is given by Eq. (23) multiplied by the discharge area. Since the thrust is independent of altitude and the discharge area does not change, we find from Eq. (23) that U/L is also independent of altitude. Substituting u_{sl} and then u_H for u in Eq. (22) and using Eq. (25) along with the fact that $U/L = \text{const}$, we obtain

$$\chi_H = \chi_{\text{sl}} \cdot \sqrt{\frac{\rho_H}{\rho_{\text{sl}}}} \tag{26}$$

Thus, we have shown that, for low-speed aircraft powered by EHD thrusters, the thrust efficiency scales approximately as the square root of the density. This result suggests that using EHD thrusters for this type of aircraft does not make much sense at high altitude.

To investigate to what extent the simple analytical equations (22) and (23) are applicable, we have calculated the ratios of analytically predicted thrust and thruster efficiency to numerically calculated $T_{\max}$ and χ (Figs. 12 and 13, respectively). Figure 13 also shows the Bondar–Bastien estimated thruster efficiency [9]:

$$\chi = \frac{u_0}{u_0 + \frac{\mu_i \cdot U}{L}} \tag{27}$$

which coincides with Eq. (22) when $V_{\text{drift}} \gg u$. As one can see, Eqs. (23) and (27) give reasonable estimates for the $T_{\max}$ and χ in almost all regions of $j_{\max}$, while Eq. (22) works only for large $j_{\max}$

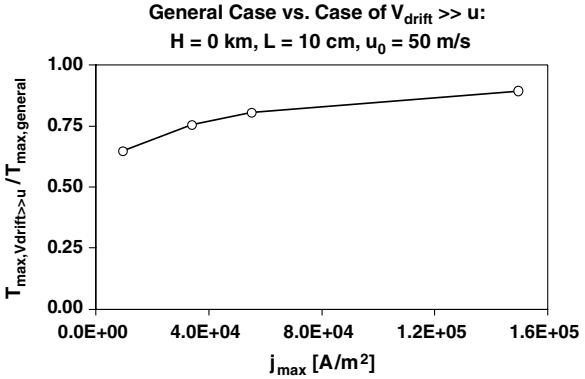

Fig. 12 Ratio of thrusts calculated by Eq. (23), the case of $V_{\text{drift}} \gg u$, and Eq. (7) at maximum current.

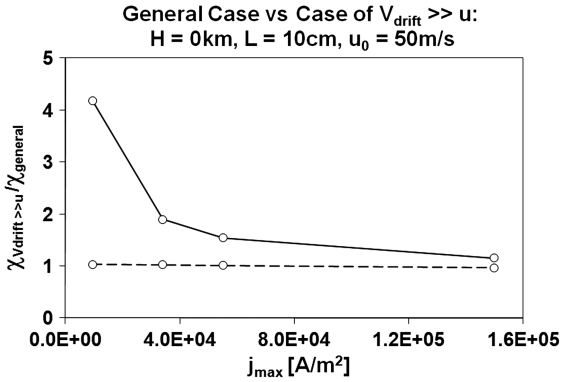

Fig. 13 Ratio of thrust efficiencies calculated for the case of $V_{\text{drift}} \gg u$, and Eqs. (8) and (9) at maximum current [solid line: Eq. (22); dashed line: Eq. (27)].

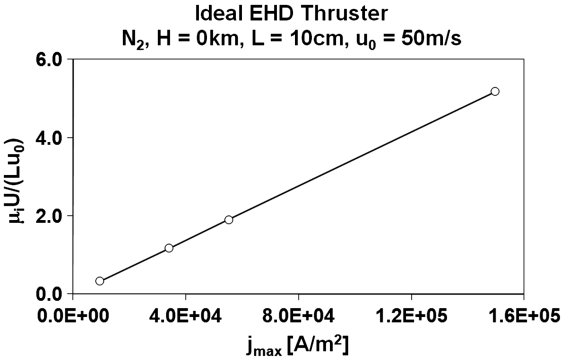

Fig. 14 Ratio of drift velocity to gas velocity at anode at maximum current.

corresponding to large V_{drift}. The ratio of ion drift velocity, $\mu_i \cdot U/L$, to u_0 is shown in Fig. 14.

The increase in temperature of gas flow due to ohmic heating by the discharge can be estimated from the law of conservation of energy:

$$W_j = W_k + W_{k,i} + \tfrac{3}{2} \cdot k \cdot \Delta T_a \cdot n_{a,0} \cdot u_0 \tag{28}$$

where

$$W_j = j_{\max} \cdot U, \qquad W_k = m_a \cdot n_{a,0} \cdot u_0 \cdot \left(\frac{u_1^2}{2} - \frac{u_0^2}{2}\right)$$

$$W_{k,i} = \frac{j_{\max} \cdot m_i}{2 \cdot e} \cdot \left(\frac{\mu_i \cdot U}{L}\right)^2$$

and the last term in the right-hand side of Eq. (28) is the internal energy that the air gains per second per unit of the discharge area as it goes through the thruster. As shown in Fig. 15, ΔT_a increases with a decrease in speed of the vehicle and with an increase in the length of the thruster; this makes perfect sense. The faster neutral gas streams through the EHD-discharge chamber, the smaller ΔT_a gets. Since

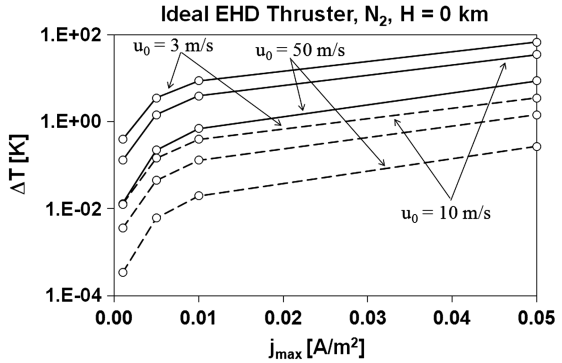

Fig. 15 An estimate for ΔT_a (solid lines: $L = 1$ m; dashed lines $L = 10$ cm).

ΔT_a is quite small, even for $L = 1$ m, the sixth assumption in Sec. II is well satisfied.

Table 1 shows the ratio of the ion drift velocity at the anode (where electrical field is largest) to the thermal velocity of neutral gas flow and $U/(P \cdot L)$ for different altitudes, gas flow velocities, and lengths of the EHD thruster. As was mentioned in Sec. II, when V_{drift}/V_{Ta} approaches unity, Eq. (5) for ion mobility becomes invalid. Since the electrical breakdown voltage of nitrogen gas is about $1.4 \cdot 10^6$ V/(m · atm) [12] (and is close to the electrical breakdown of air [14]), electrical breakdown would most likely appear before Eq. (5) became invalid (Table 1). Therefore, the results corresponding to the case where $V_{\text{drift}}/V_{Ta} > 1$ should be considered from an illustrative point of view only.

IV. Conclusions

A 1-D model of an ideal EHD thruster has been presented. It has been shown that the ion current in an ideal EHD thruster cannot exceed the space-charge-limited current $j_{\max}$; therefore, the thrust of such a thruster cannot exceed the thrust corresponding to this current. It has been shown that thrust and thrust efficiency work against each other in EHD thrusters: the larger the thruster current (larger thrust), the smaller the thruster efficiency. It has also been shows that, at high altitudes, the performance of EHD thrusters (thrust and thrust efficiency) drops very fast due to a rapid increase in ion mobility with elevation. Moreover, at high altitudes, the electrical breakdown of air can limit the ion current even more drastically than the electrical charge, leading to a significant decrease in the thrust. Therefore, using EHD thrusters at altitudes greater than 5 km is apparently unrealistic. The model shows that maximum thrust cannot exceed 20–30 N/m^2 at sea level, even at breakdown voltage; thus, this also does not look very encouraging. Since the model is ideal and does not take into account numerous other factors that can negatively impact the performance of EHD thrusters even more, it may be concluded that the idea of using the EHD ionic wind pump effect for thruster application is rather dim.

References

[1] Hauksbee, F., *Physico-Mechanical Experiments on Various Subjects*, 1st ed., R. Brugis, London, 1709, pp. 46–47.

[2] Robinson, M., "A History of the Electric Wind," *American Journal of Physics*, Vol. 30, No. 5, 1962, pp. 366–372.

Table 1 V_{drift}/V_{Ta} and E/P [V/(m · atm)]

	$H = 0$ km, $L = 0.1$ km						$L = 1$ m		$H = 20$ km, $L = 0.1$ m	
	$u_0 = 3$ m/s		$u_0 = 10$ m/s		$u_0 = 50$ m/s		$u_0 = 50$ m/s		$u_0 = 50$ m/s	
A/m^2	V_{drift}/V_{Ta}	E/P	V_{drift}/V_{Ta}	E/P	V_{drift}/V_{Ta}	E/P	V_{drift}/V_{Ta}	E/P	V_{drift}/V_{Ta}	E/P
0.001	0.07	8.63×10^4	0.12	1.80×10^5	0.13	2.09×10^5	0.34	5.02×10^5	0.61	7.85×10^5
0.005	0.022	3.10×10^5	0.29	4.56×10^5	0.29	4.58×10^5	0.89	1.36×10^6	1.53	2.04×10^6
0.01	0.34	5.02×10^5	0.42	6.06×10^5	0.40	6.15×10^5	1.29	2.02×10^6	2.22	2.98×10^6
0.05	0.89	1.36×10^6	0.92	1.45×10^6	0.74	1.09×10^6	2.97	4.70×10^6	5.12	6.99×10^6

doi:10.1119/1.1942021
[3] Rickard, M., Dunn-Rankin, D., Weinberg, F., and Carleton, F., "Characterization of Ionic Wind Velocity," *Journal of Electrostatics*, Vol. 63, Nos. 6–10, 2005, pp. 711–716. doi:10.1016/j.elstat.2005.03.033
[4] Jewell-Larsen, N. E., Ran, H., Zhang, Y., Schweibert, M., Schwiebert, M. K., Tessera, K. A. H., and Mamishev, A. V., "Electrohydrodynamic (EHD) Cooled Laptop," *Proceedings of the 25th IEEE SEMITHERM Symposium*, IEEE Publ., Piscataway, NJ, 2009, pp. 261–266.
[5] Stuetzer, O. M., "Ion Transport High Voltage Generators," *Review of Scientific Instruments*, Vol. 32, No. 1, 1961, pp. 16–22. doi:10.1063/1.1717134
[6] Fantel, H., "Major de Seversky's Ion-Propelled Aircraft," *Popular Mechanics*, Aug. 1964, 58–196.
[7] Christenson, E. A., and Moller, P. S., "Ion-Neutral Propulsion in Atmospheric Media," *AIAA Journal*, Vol. 5, No. 10, 1967, pp. 1768–1773. doi:10.2514/3.4302
[8] Robinson, M., "Movement of Air in the Electric Wind of the Corona Discharge," Armed Services Technical Information Agency Rept. AD-262A30, Arlington, VA, 1961.
[9] Bondar, H., and Bastien, F., "Effect of Neutral Fluid Velocity on Direct Conversion From Electric to Fluid Kinetic Energy in an Electro-Fluid-Dynamic (Efd) Device," *Journal of Physics, D: Applied Physics*, Vol. 19, No. 9, 1986, pp. 1657–1663. doi:10.1088/0022-3727/19/9/011
[10] Singhal, V., and Garimella, S. V., "Influence of Bulk Fluid Velocity on the Efficiency of Electrohydrodynamic Pumping," *Transactions of the ASME*, Vol. 127, No. 3, 2005, pp. 484–494. doi:10.1115/1.1843166
[11] Rickard, M., Dunn-Rankin, D., Weinberg, F., and Carleton, F., "Maximizing Ion-Driven Gas Flows," *Journal of Electrostatics*, Vol. 64, No. 6, 2006, pp. 368–376. doi:10.1016/j.elstat.2005.09.005
[12] Raizer, Y. P., *Gas Discharge Physics*, Springer, New York, 2001, pp. 24–25.
[13] Tammet, H., Iher, H., and Salm, J., "Spectrum of Atmospheric Ions in the Mobility Range of 0.32–3.2 $\mathrm{cm}/(\mathrm{V}\cdot\mathrm{s})$," *Acta et Commentationes Universitatis Tartuensis*, Vol. 947, 1992, pp. 35–49, http://ael.physic.ut.ee/KF.public/sci/publs/acta/947/D.PDF [retrieved 2011].
[14] Akamine, V., Matsuoka, S., Chiba, M., and Hidaka, K., "Electrical Breakdown Characteristics of Nitrogen and Air at Cryogenic Temperatures in Quasi-Uniform Electric Field," *Electrical Engineering in Japan*, Vol. 132, No. 4, 2000, pp. 28–33. doi:10.1002/1520-6416(200009)132:4<28::AID-EEJ4>3.0.CO;2-J

J. Blandino
Associate Editor